Supplementary Information

1. Insignificance of strain variety and inoculant source density for slow-fast transition variation

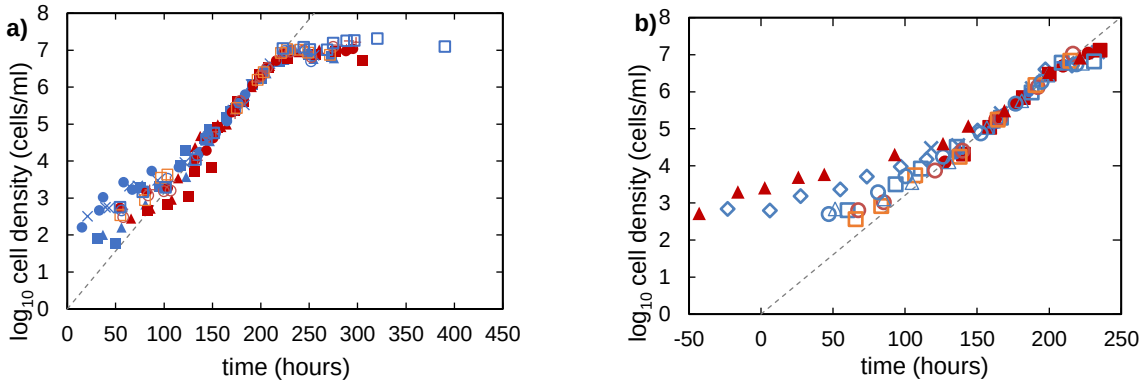

Figure S1. AX3 (a) and AX4 (b) axenic strain proliferation kinetics. Different symbols indicate different samples. Dashed line indicates the best alignment of exponential range data (from approximately 1×10^4 to 5×10^6 cell/ml) to a single exponential growth law by time translation of each run. Time zero is arbitrary. Red points indicate samples prepared from the high exponential density sources: 4×10^6 to 8×10^6 cells/ml for AX3 and 1.2×10^6 to 3×10^6 cells/ml for AX4. Blue symbols indicate the samples prepared from lower exponential density sources: 5×10^4 to 3×10^5 cells/ml for AX3 and 2×10^5 to 6×10^5 cells/ml for AX4. Counting uncertainty estimates given in Material and Methods Sec. 3.

Comparing Figures. S1 a) and b) we see no noticeable difference in the transition variation between these two axenic strains.

Brock and Gomer[1] have reported a proliferation suppression factor at high densities in the log phase. We see from Figure S1 b that the variation in the growth behavior we find does not depend on the source density to an extent that would indicate the involvement of the Brock-Gomer suppressor factor.

2. The search for a lagless strain

Previously,[2] we discussed the possibility of obtaining a lagless *D. discoideum* strain after seeing such behavior. In searching for examples of this lagless strain, we examined lines derived from frozen samples of the original strain used in the earlier work as well as material provided by the Dicty Stock Center. In no cases could we establish a consistent lagless behavior through repeated culture passages.

3. Ensuring culture consistency

As a precaution to combat possible bacterial contaminations, we used syringe filtered PenStrep. For the observations plotted in Figures 1a and 1b we kept the room lights off in our culture room when it was not in use. We kept the lights on at all times, however, in later experiments in order to suppress any possible effects of lighting on cell growth (such as entrainment of circadian rhythms)[3]. Our clean table for cell culture was kept sterile by continuously running ultraviolet lights when not in use. Since the experiments presented here were performed over a few years, we accounted for the possible effects of extended culturing by using fresh cells from the Dicty Stock Center and newly thawed out cells from our frozen stock. The slow-to-fast

transition effect persisted, even after continually culturing the cells for a year. In no case have we noticed any systematic variation or any change in growth kinetics.

4. Unimportance of rare bacterial contamination

Next, we considered the possibility that a low-level bacterial infection might retard growth at low densities and that *D. discoideum* might combat this collectively, eventually winning out, thereby producing a lagging effect. We disregarded rare (about one in a hundred) results where an infection appeared in a sample and overtook a culture. Contaminations that would escape detection in this manner specifically concerned us. Rarely, we found very low levels of a strain of *E. coli* bacteria in our cultures. Through colony growth assays on agar plates, we established that this *E. coli* strain was resistant to the penicillin and streptomycin antibiotics we used for *D. discoideum* growth, but highly susceptible to tetracycline. We tested the effect of these occasional contaminations on cell growth and the lag phase duration by performing an experiment with the turbidity point setup (see Materials and Methods Sec 4) with small vials (volume 0.6 ml) dosed with antibiotics at variable strengths. For each dose, we prepared eight experimental samples, two control samples with no *D. discoideum* cells, and three samples at 10^4 cells/ml for exponential growth rate estimation. As shown in Fig. S2, these experiments revealed no significant difference in doubling times in the exponential growth phase up to the standard doses of tetracycline (to check for *E. coli* effects) doses or penicillin/streptomycin (our usual combination antibiotic). Similarly, there was no change in the lagtime for either antibiotic up to the standard dose. At the highest dose of tetracycline (four times the standard dose), the lag time was severely reduced with the application. We conclude that there was no sign of bacterial contamination, including *E. coli*, in our reported measurements.

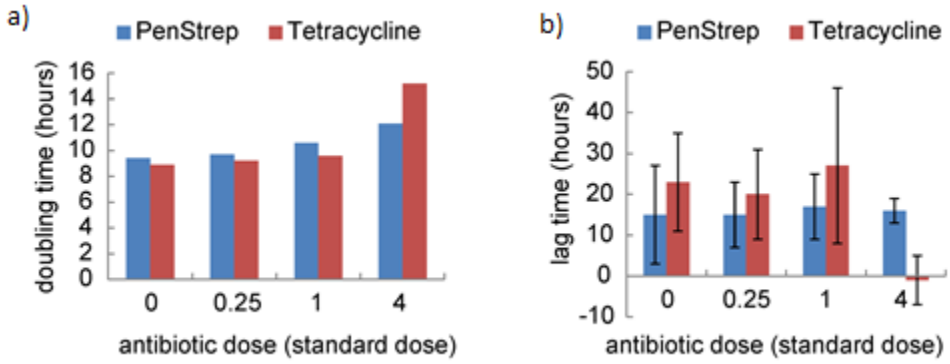

Figure S2. No sign of the effect of antibiotics up to standard doses on a) cell culture or b) the Allee effect. We conclude that bacterial contamination is unimportant

As an additional contamination control, we spotted agar plates from 20 small volume (0.6ml) samples that had grown into the exponential growth phase. We observed no bacterial growth, although the plates showed ready sensitivity to *E. coli* as expected. Of these specimens, we selected the longest lagging sample for intensive microscopic inspection and found no traces of *E. coli* or any other contaminants. Therefore, from all this evidence, we conclude that a low-level bacterial contamination does not cause the lagging behavior we observe.

5. Previous conditioned medium experiments

Earlier,[2] we performed 8 conditioned media experiments in large 30 ml volume samples, with initial cell densities between 2×10^3 and 7×10^3 cells/ml and growth medium prepared by mixing equal amounts of fresh and CM (obtained from the 10^6 cells/ml samples). Now, having more accurately determined the range in which the slow-to-fast growth transition occurs, we note that initial densities in the previous experiments were very close to the transition density 10^4 cells/ml, there were only 6 samples and the fast growth rate estimates had a relatively large uncertainty. We have since quantitatively established a large variation in growth kinetics (as reported in this work) and therefore decided to perform a much more extensive set of conditioned media measurements as reported in the main text.

6. The unimportance of variation in the phase of the cell cycle.

To evaluate the effect of variable positions in the cell cycle on variations in lagging, we performed a simulation which began by assuming 60 cells in a 0.6ml vial – matching the initial density of our turbidity point experiments. We allowed the cells to divide at a time-independent rate (following Poisson statistics) with the following important caveat: for each cell, we tracked the time since its last division and only allowed a division if that time exceeded T_0, the minimum time interval needed to complete the cell cycle. We estimated T_0 from two sources: culture recommendations[4] explain that the fastest doubling time for log phase growth (when grown on bacteria) is 4 hours and measurements of the cell cycle of the AX2G strain[5] found a cell cycle time of approximately 12 hours. We took this as an upper limit for T_0. Running the simulations repeatedly for these two extremes of T_0 - 4 and 12 hours - we found standard deviations in the times it took to reach the log phase cell density of 1.5 and 1.9 hours, respectively. This is considerably shorter than the variations we noticed in Figure 1e. We conclude that cell cycle variation does not account for the observed diversity in lagging.

7. Calculation of the variation in lag times due to sampling noise in the initial cell density

In the main text (Fig. 1a) we showed that the cells are growing exponentially in the lag phase with a typical doubling time T_{slow} = 20 hours. Therefore, in the lag phase the cell number after time *t* is:

$$n(t) = n_0 2^{t/T_{slow}}$$

The lag times were obtained by the method shown in Fig. 2d i.e., by matching the actual growth (which includes the lag phase) and pure exponential (log) growth started after t_{lag} at the crossover cell density $n(t = t_x) = n_x$. The equations of both curves are (with T_{fast} having by a typical value of 11 hours) given by:

$$n_{lag}(t) = n_0 2^{t/T_{slow}},\ \ n_{log}(t) = n_0 2^{(t-t_{lag})/T_{fast}}$$

At the crossover from slow to fast growth we have $n_{lag}(t_x) = n_{log}(t_x)$:

$$n_0 2^{t_x/T_{slow}} = n_0 2^{(t_x-t_{lag})/T_{fast}}$$

$$t_x - t_{lag} = \frac{T_{fast}}{T_{slow}} t_x$$

$$t_{lag} = t_x \left(1 - \frac{T_{fast}}{T_{slow}}\right) = t_x \left(\frac{T_{slow} - T_{fast}}{T_{slow}}\right)$$

Now, we want to express t_x as a function of the initial density n_0:

$$t_x = T_{slow}\, ln\left(\frac{n_x}{n_0}\right) \,/\ln(2)$$

and we have:

$$t_{lag} = \frac{\left(T_{slow} - T_{fast}\right)}{ln(2)} ln\left(\frac{n_x}{n_0}\right)$$

Finally, if our uncertainty in the initial density for our small volume measurements was due to the root N Poissonian sampling noise of $\sigma_{N_0} = 8$, ($N_0 = n_0 V = 60\ cells$, where V is the volume) the uncertainty in the lag times is given by the error propagation formula:

$$\sigma_{t_{lag}} = \left|\frac{\partial t_{lag}}{\partial N_0}\right| \sigma_{N_0} = \frac{\left(T_{slow} - T_{fast}\right)}{N_0\ ln\ 2} \sigma_{N_0} = 1.7\ hours$$

The 2σ interval covers a range of 3.4 hours. However, Fig. 1e shows that the observed variation was much greater (26 hours). For our 25 ml volume samples (Figures 1a and 1b), the spread should be negligible (0.3 hours) because of the much greater sampling size ($N_0 = 2500 \pm 50$ cells); however, as we have seen, a comparable range of observed lag time persists. Therefore, we conclude that the natural uncertainties in the inoculation densities cannot account for the observed range of variation in lag times.

8. Statistical significance tests of conditioned media experiments

Here we describe tests for the potential difference between the mean lagging time in conditioned media experiments. We start with a null hypothesis: the means of lagging times in each set of conditioned media experiments (taken from the same source; columns in Fig. 4) are the same. The means are compared using the Welch Two Sample t-test, as follows. First the test statistic t is defined as the difference between the mean lagging times normalized by the variance of two samples:

$$t = \frac{\overline{x_1} - \overline{x_2}}{S_{x_1 - x_2}}, \quad S_{x_1 - x_2} = \sqrt{\frac{{s_1}^2}{n_1} + \frac{{s_2}^2}{n_2}}$$

where s_1 and s_2 are the standard deviations and $\overline{x_1}$ and $\overline{x_2}$ are the means of the samples x_1 and x_2. The distribution of the test statistic is then approximated as an ordinary Student's t distribution with the degrees of freedom parameter calculated by the Welch-Satterthwaite equation:

$$df = \frac{\left(\frac{{s_1}^2}{n_1} + \frac{{s_2}^2}{n_2}\right)^2}{\frac{\left(\frac{{s_1}^2}{n_1}\right)^2}{n_1 - 1} + \frac{\left(\frac{{s_2}^2}{n_2}\right)^2}{n_2 - 1}}$$

Then, we compared the lagging times obtained between pairs of experiments with different amounts of conditioned media by calculating the following p-value: the probability of obtaining a test statistic at least as extreme as the one observed, assuming that the null hypothesis is true. In other words, large p-values[6] imply that we cannot reject the null hypothesis. The comparison between the experiments with different amounts of conditioned media from Fig. 4 in the main text is given in Tables S1 and S2.

Table S1. Conditioned media taken from cells below the transition, at 2000 cells/ml cell density.

p-value	0.1% CM	5% CM	100% CM
0% CM	0.45	0.72	0.36
0.1% CM	-	0.22	0.58
5% CM	-	-	0.25

Table S2. Conditioned media taken from cells above the transition at 3×10^5 cells/ml (30 samples for each experiment; left entries) and 5×10^5 cells/ml (13 samples for each experiment; right entries).

p-value	0.1% CM		5% CM		100% CM	
0% CM	0.08	0.16	0.93	3×10^{-4}	2.2×10^{-16}	5×10^{-3}
0.1% CM	-		0.17	7×10^{-3}	1.8×10^{-7}	0.02
5% CM	-		-		6.2×10^{-5}	0.16

These tables show us first that the null hypothesis cannot be rejected if the conditioned media is taken from the cells below the transition and can be rejected if the conditioned media is taken from cells above the transition, when comparing the means of the lagging times between samples with 0% and 100% of conditioned media. The experiments performed with conditioned media taken from cells at 3×10^5 cells/ml had three times the number of samples, which is reflected by much smaller p-values in comparing 0% and 100% conditioned media experiments.

9. Estimation of chemical signal threshold and secretion rates per cell

For chemical signal concentrations below the threshold $c < c_x$, $n(t)$ is given by:

$$n(t) = n_0 e^{\gamma_{slow} t}$$

Integrating Eqn. 3 of subsection 6 of the section 2 of the main text, the cell density and growth factor concentration at the transition are given by:

$$c(t = t_x) = c_x = \frac{v n_0}{\gamma_{slow}} (e^{\gamma_{slow} t_x} - 1)$$

$$n(t = t_x) = n_0 e^{\gamma_{slow} t_x}$$

where t_x is the time for the transition. Combining equations, we have:

$$c_x = \frac{\upsilon}{\gamma_{slow}}(n_x - n_0) \approx \frac{\upsilon}{\gamma_{slow}} n_x$$

for $n_x \gg n_0$ as is the case with $n_x \approx 10^4$ cells/ml and $n_0 \approx 100$ cells/ml.

Our estimate for υ is based on an estimation of production rate of extracellular secretions from two different cellular systems: 1) the production of cAMP of starved *D. discoideum* and 2) the production of fibroblast growth factor by 3T3 cells (which are derived from mouse embryos). First, in the *D. discoideum* starvation system authors in Ref. (7) monitored extracellular cAMP production from a high-density system which was pulsatile in nature. We averaged the production rate from their work, giving us the high value of 9×10^3 molecules/ (cell s). Second, although it was not intended to be a quantitative measurement of the growth factor secretion rate ν, authors in Ref. (8) observed the production of fibroblast growth factor due to heat shock. Assuming that a single standard size petri dish was used and estimating cellular density at confluence, we find a production rate of 400 molecules/ (cell s).

10. Cluster generated endocrine and paracrine models – stochastic simulations

We implemented stochastic versions of cluster-generated endocrine and paracrine models as follows. MATLAB with SimBiology (Mathworks, US) was used to model this system as shown in Fig. S3. In each model, we consider cells to be in one or two states (single or clustered).

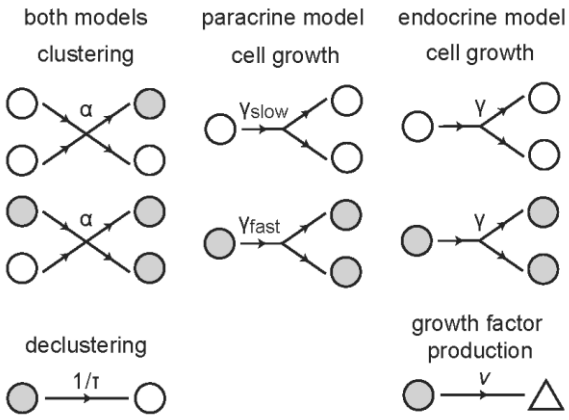

Figure S3. Stochastic cluster-generated models. Both endocrine and paracrine models include the clustering term described by the clustering rate constant α. This constant was estimated using the model for particle clustering based on velocity-gradient flocculation (see main text) and was estimated to about $\alpha = 10^{-9}$ s^{-1}. Clustered cells are shown in gray while single cells are shown in white circles. Growth factors are shown as white triangles.

[1] D.A. Brock and R.H. Gomer, ``A secreted factor represses cell proliferation in Dictyostelium,'' Development, **132**, 4553 (2005).

[2] C. Franck, W. Ip, A. Bae, N. Franck, E. Bogart and T. T. Le, "Contact-mediated cell-assisted cell proliferation in a model eukaryotic single-cell organism: an explanation for the lag phase in shaken cell culture.," Phys. Rev. E **77**, 041905 (2008).

[3] We appreciate this suggestion from an anonymous referee.

[4] P. Fey, A.S. Kowal, P. Gaudet. K.E. Pilcher, and R. L. Chisholm, ``Protocols for growth and development of Dictyostelium discoideum,'' Nature Protocols **2**, 1307 (2007).

[5] T. Muramoto and J.R. Chubb, J. R. ``Live imaging of the Dictyostelium cell cycle reveals widespread S phase during development, a G2 bias in spore differentiation and a premitotic checkpoint,'' Development **135**, 1647 (2008).

[6] S. N. Goodman, "Toward Evidence-Based Medical Statistics. 1: The P Value Fallacy.," Annals of Internal Medicine, **130**, 995 (1999).

[7] G. Gerisch and U. Wick, "Intracellular oscillations and release of cyclic AMP from Dictyostelium cells," Biochem and Biophys Research Comm., **65**, 364 (1975).

[8] A. Jackson, S. Friedman, X. Zhan, K. A. Engleka, R. Forough and T. Maciag, "Heat shock induces the release of fibroblast growth factor 1 from NIH 3T3 cells," Proc. Natl. Acad. Sci. USA, **89**, 10691 (1992).